Electromagnetic-Actuated High-Resolution Tactile Device With Actuating and Sensing Capabilities

Yuan Guo, *Member, IEEE*, Chao Shang, Qianqian Tong, *Member, IEEE*, Yuru Zhang, *Senior Member, IEEE*, Zhengchun Peng, and Dangxiao Wang, *Senior Member, IEEE*

***Abstract*—Tactile devices with both actuating and sensing capabilities provide an intuitive way to convey tactile information. It however remains a challenge to compact the actuator and sensor array while avoiding the sensor obstructing the actuator motion. Here, we report an actuating–sensing integrated tactile device with a 3-mm resolution, in which magnetic actuators and piezoresistive sensors are compactly interlaced in a reticular layout with the sensors sandwiched between two membrane brackets. The reticular sandwich structure effectively prevents sensors from interfering with actuators, while shortening the spacing between the actuator and sensor to meet the requirements of both the actuator and the sensor within the compact contact area of a fingertip. When touched, the resistance of the distributed sensors is changed and mapped to the drive current of the accessible actuators. This work principle enables the proposed tactile device to modulate the actuators through touching location and pressure, and to reproduce tactile patterns or vibrations for the user. Experimental results show that the tactile device with tactile display and tactile sensing can be used for tactile communication between users or the user and virtual character.**

Manuscript received 30 July 2023; revised 26 October 2023; accepted 3 December 2023. Date of publication 19 December 2023; date of current version 17 October 2024. Recommended by Technical Editor H. Yu and Senior Editor G. Alici. This work was supported by the National Natural Science Foundation of China under Grant 61973016, Grant 62002185, and Grant 62373021. *(Yuan Guo and Chao Shang contributed equally to this work.) (Corresponding authors: Dangxiao Wang; Zhengchun Peng.)*

Yuan Guo and Yuru Zhang are with the State Key Lab of Virtual Reality Technology and Systems, and School of Mechanical Engineering and Automation, Beihang University, Beijing 100191, China (e-mail: guoyuanbh@buaa.edu.cn; yuru@buaa.edu.cn).

Chao Shang and Zhengchun Peng are with the Center for Stretchable Electronics and Nano Sensors, Key Laboratory of Optoelectronic Devices and Systems of Ministry of Education, School of Physics and Optoelectronic Engineering, Shenzhen University, Shenzhen 518060, China (e-mail: shangc0315@foxmail.com; zcpeng@szu.edu.cn).

Qianqian Tong is with the Department of Strategic and Advanced Interdisciplinary Research, Peng Cheng Laboratory, Shenzhen 518055, China (e-mail: tongqq@pcl.ac.cn).

Dangxiao Wang is with the State Key Lab of Virtual Reality Technology and Systems, and School of Mechanical Engineering and Automation, Beihang University, Beijing 100191, China, and also with the Department of Strategic and Advanced Interdisciplinary Research, Peng Cheng Laboratory, Shenzhen 518055, China (e-mail: hapticwang@buaa.edu.cn).

This article has supplementary material provided by the authors and color versions of one or more figures available at https://doi.org/10.1109/TMECH.2023.3340564.

Digital Object Identifier 10.1109/TMECH.2023.3340564

***Index Terms*—Magnetic actuator, piezoresistive sensor, tactile device, tactile display, tactile sensing.**

I. Introduction

MECHANORECEPTORS embedded in the skin can dynamically sense multiple interactive information in real time, such as pressure, location, and temperature [1], [2], [3], [4]. These tactile information can be effectively conveyed and reformulated by tactile devices to induce tactile perception in the form of mechanoreceptor stimulation [5], [6], [7], [8], [9]. In the past decade, tactile devices with both tactile display and tactile sensing (i.e., actuating–sensing integrated tactile devices) have been developed and found applications in areas as diverse as virtual reality [10], [11], wearable interfaces [12], [13], [14], texture display [15], and robotics [16], [17], [18]. These tactile devices feature both actuation and sensing functions, which provide a potential way for the user to communicate with the other one or a virtual character through tactile information [19], [20].

For an actuating–sensing integrated tactile device, the actuating and sensing capabilities within a compact contact area are crucial to realize real-time tactile interaction, which in principle requires at least one actuator and one sensor in a certain contact area (such as a circular area of 34.32 mm^2 for index [21]) between the fingertip and tactile device (called spatial registration). With this characteristic, when the fingertip touches any position of the tactile device, the sensors can acquire the position and pressure of the finger, and then the corresponding actuators formulate texture patterns or vibrations for the user.

For existing actuating–sensing integrated tactile devices, sensors are widely placed on top of actuators [16], [22], [23], [24]. With this layout, the fingertip can simultaneously cover both the actuator and the sensor, but the presence of the upper sensor would block the movement of the actuator, thereby attenuating tactile stimulation produced by actuators and affecting the users' interactive experience. To avoid the sensor obstructing the actuator motion, Phung et al. [25] cut holes in the sensor layer to expose the actuator, whereas these holes result in the uneven surface of the tactile device, which is not conducive to sliding on the tactile device. More importantly, its spatial resolution (16 mm) is larger than the diameter (6.6 mm [21]) of the circular contact area, which does not meet the requirement of

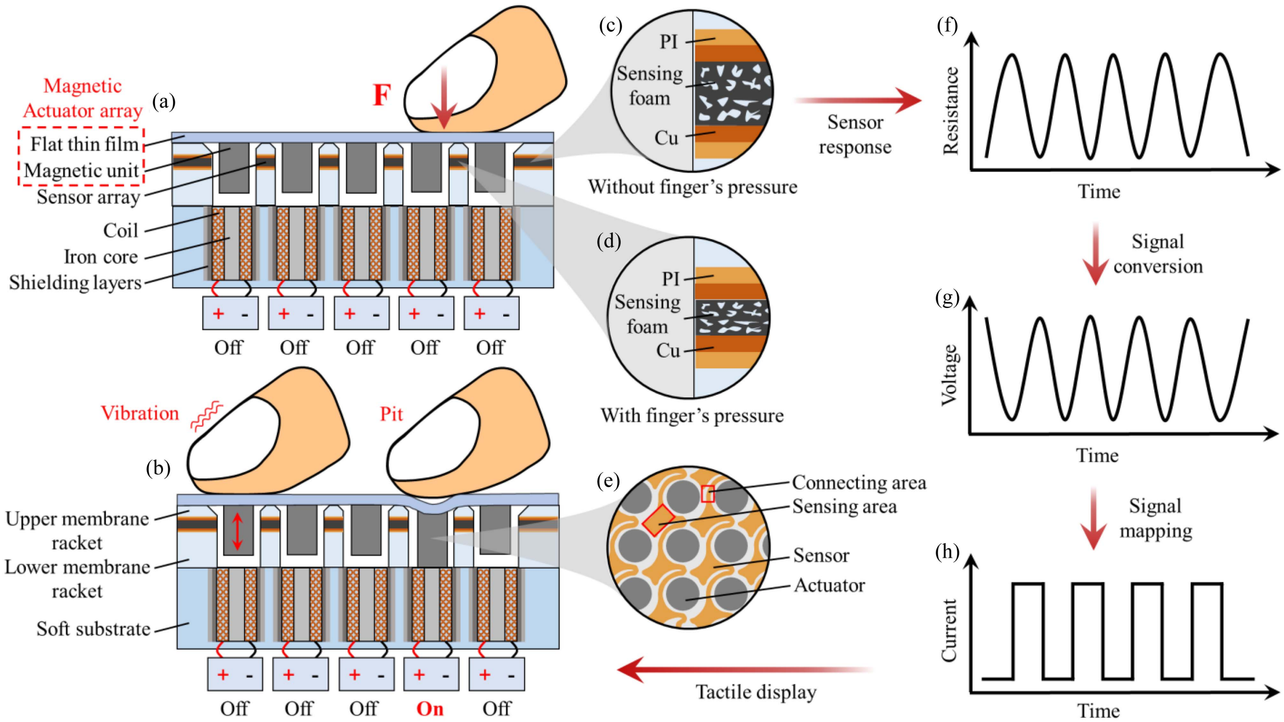

Fig. 1. Schematic illustration of the design and operating principle. (a) At the initial state, the thin film is flat. (b) Under the drive current, the magnetic actuator moves up and down at a certain frequency (vibration) or moves downward (forming a pit). (c) And (d) internal states of the sensor without/with finger's pressure. (e) Reticular layout of actuators and sensors. (f) Resistance changes under the applied pressure. (g) Resistance variation is converted to the voltage variation. (h) Voltage variation is mapped to the drive current.

actuating–sensing spatial registration. As the authors reported, it is difficult to activate the actuator and sensor within the compact contact area of a fingertip [25].

In this article, we present a high-resolution tactile device with both tactile display and tactile sensing, which can meet the requirement of both the actuator and the sensor within the compact contact area of a fingertip while avoiding the sensor obstructing the actuator motion. The main contributions of this article are summarized as follows.

1) The novel reticular sandwich structure is proposed for the actuating–sensing integrated tactile device, in which the magnetic actuators and piezoresistive sensors are compactly interlaced in a reticular layout with the sensors sandwiched between the membrane brackets. The proposed reticular sandwich structure effectively prevents the piezoresistive sensors from affecting the magnetic actuators, and endows the proposed tactile device with a smooth and flat surface, providing a good interactive experience for users during finger exploration.
2) The serpentine traces are employed to accommodate and match the shape of the magnetic actuator, which effectively miniaturizes the sensor array and shortens the spacing between the actuator and sensor. Moreover, along with using the reticular sandwich structure, we further reduce the spacing between adjacent actuators, resulting in a resolution of 3 mm for the tactile device.
3) Three representative interaction scenarios are designed to verify the functions of the proposed actuating–sensing integrated tactile device, and the experiments show that our tactile device has the potential to be used across a wide range of applications pertaining to intelligent vehicles, virtual reality, teleoperation, social media, and other fields.

II. Design and Work Principle

In the proposed actuating–sensing integrated tactile device, the actuating is achieved through the magnetic force between the coil and magnetic unit, and the sensing is realized by the piezoresistive effect. To meet the requirement of the spatial registration, the spacing and the size of both the actuator and sensor should be small enough to be embedded within the compact contact area of a fingertip. Based on the fabrication technique proposed in our previous work [26], we developed a 1.5-mm magnetic actuator. As depicted in Fig. 1(a) and (b), the magnetic actuator array is made up of soft thin film and magnetic units, which is used to provide texture patterns or vibration. The sensor array consisting of two stacked sensing layers is fabricated with sensing foams, polyimide (PI) sublayers, and Cu sublayers [see Fig. 1(c) and (d)] for perceiving the contact position and pressure [27].

To effectively prevent the piezoresistive sensors from affecting the magnetic actuators, the magnetic actuators and piezoresistive sensors are compactly interlaced in a reticular layout with the sensors sandwiched between the upper and lower membrane brackets (as detailed in Text S1 and Fig. S1, Supplementary material). In addition, the upper part of the hole on the upper membrane bracket is designed as the frustum of a cone [see Fig. 1(a)], resulting in a larger spacing between adjacent magnetic actuators on the lower surface of the upper membrane bracket compared to the upper surface. Therefore, when the size of the piezoresistive sensor is determined, the sensor array is arranged on the lower surface of the upper membrane bracket (i.e., sandwiched in the upper and lower membrane brackets), which can reduce the spacing between the adjacent magnetic actuator, thereby improving the resolution of the tactile device.

To accommodate and match the shape of the magnetic actuator, the morphed serpentine traces are used to miniaturize the piezoresistive sensor array (as detailed in Text S1 and Fig. S1, Supplementary material). This morphed serpentine trace takes advantage of the cambered area in the magnetic actuator array, and the spacing between the tilting and horizontal/vertical directions of the magnetic actuators is utilized as the sensing and connecting area [see Fig. 1(e)]. This approach effectively shortens the spacing between the actuator and sensor, and improves the spatial resolution of the tactile device (3 mm), so that the fingertip can simultaneously cover two actuators and two sensors.

When interacting with the proposed tactile device, the resistance variation of the sensor is mapped to the drive current of the accessible actuator. As depicted in Fig. 1(c), the size of the randomly distributed pores in the sensing foam remains constant before the pressure is applied, and the resistance of the sensing foam is fixed. Under the pressure of the fingers, the pores are squeezed smaller to form new conduction paths, effectively reducing the resistance [see Fig. 1(d)]. As shown in Fig. 1(f) and (g), the resistance variation is converted to the voltage variation by the sampling circuit of the control system. The voltage signal is mapped to the drive current of the control system to activate the coil [see Fig. 1(h)], and the desired mapping relationship can be defined according to the different interactive scenarios.

The magnetic force varies with the drive current of the coil. When a constant drive current is applied to the coil, the magnetic actuator moves down and formulates a pit on the proposed tactile device. The formulated pit maintains a certain depth until the drive current is off. Under the energization of the pulsating drive current, the magnetic unit moves up and down periodically in accordance with the frequency of the pulsating drive current. Depending on the duration of the drive current, the magnetic actuator possesses two motion states: nonvibration state or vibration state [see Fig. 1(b)], which allows the proposed tactile device to formulate a certain pattern for finger exploration or directly provide vibration stimulation to the finger. Once the applied pressure is released, the pores in the sensing foam return to their original shape, and the resistance is restored to its original value. Meanwhile, the drive current becomes zero and the magnetic actuator moves upward under the recovery force of the soft thin film. The formulated pit disappears and the thin film returns to a flat state. Benefiting from this work principle, the proposed tactile device can control the actuator through the sensing signals, which can be used for tactile communication between users or the user and virtual character.

III. Overall Architecture

A. Device Fabrication

To fabricate the actuating–sensing integrated tactile device, we need to prepare the magnetic actuator array, piezoresistive sensor array, membrane bracket, and soft substrate. Among them, the magnetic actuator array, membrane bracket, and soft substrate are prepared by the molding technique (see the fabrication process in Text S2, Text S4, Fig. S2, and Fig. S4, Supplementary material). The piezoresistive sensor array with morphed serpentine traces is fabricated by laser direct writing technology (see the fabrication process in Text S3 and Fig. S3, Supplementary material). These miniaturized magnetic actuators and serpentine sensors enable the development of high-resolution tactile devices.

After the fabrication of the above components, the coils, iron cores, and shielding layers are successively assembled in the soft substrate [see Fig. 2(a) and (b)]. The coil is made of 0.18-mm copper wire, with a height of 10 mm and an outer diameter of 2.85 mm. The iron core with a height of 10 mm and a diameter of 1 mm (permalloy 1J50, Suzhou Haichuan Rare Metal Products Co., Ltd, China) is inserted into the coil to enhance the excitation magnetic field. To reduce the magnetic interference between adjacent coils, the shielding layers consisting of 0.05-mm pure iron and 0.05-mm permalloy are wrapped around each coil.

Next, two sensing layers are stacked orthogonally together to form the 6×6 sensor array, which transmits the sensing signals for rows and columns [see Fig. 2(a)]. The sensor array is sandwiched between the upper and lower membrane brackets [see Fig. 2(b)]. Then, a 5×5 magnetic actuator array is integrated into the holes of the upper and lower membrane brackets (see Fig. S6c, Supplementary material). The upper membrane bracket, lower membrane bracket, and soft substrate are glued together using a silicon adhesive (Smooth-On Inc., USA), assembling a whole tactile device [see Fig. 2(b); and Fig. S7, Supplementary material). Benefiting from the sandwich structure, the sensor array does not block the motion of magnetic actuators, and the resistance of the sensor array can be easily changed under the applied pressure.

As shown in Figs. 1(e) and 2(b), the magnetic actuators and piezoresistive sensors are compactly interlaced in a reticular layout. Compared with other layouts, the reticular sandwich structure makes full use of the spacing between the actuator and sensor, which effectively improves the resolution of the tactile device (see Table S1, Supplementary material). Moreover, this reticular sandwich structure endows the proposed tactile device with a smooth and flat surface, which can provide a good interactive experience for users during finger exploration.

B. Control System

To characterize the correspondence between the magnetic actuator and adjacent sensors, we set that the activation state of the magnetic actuator depends on the average resistance change of the four sensors around this magnetic actuator (Fig. S8, Supplementary material). A real-time sampling circuit is adopted to monitor the resistance variation of all sensors

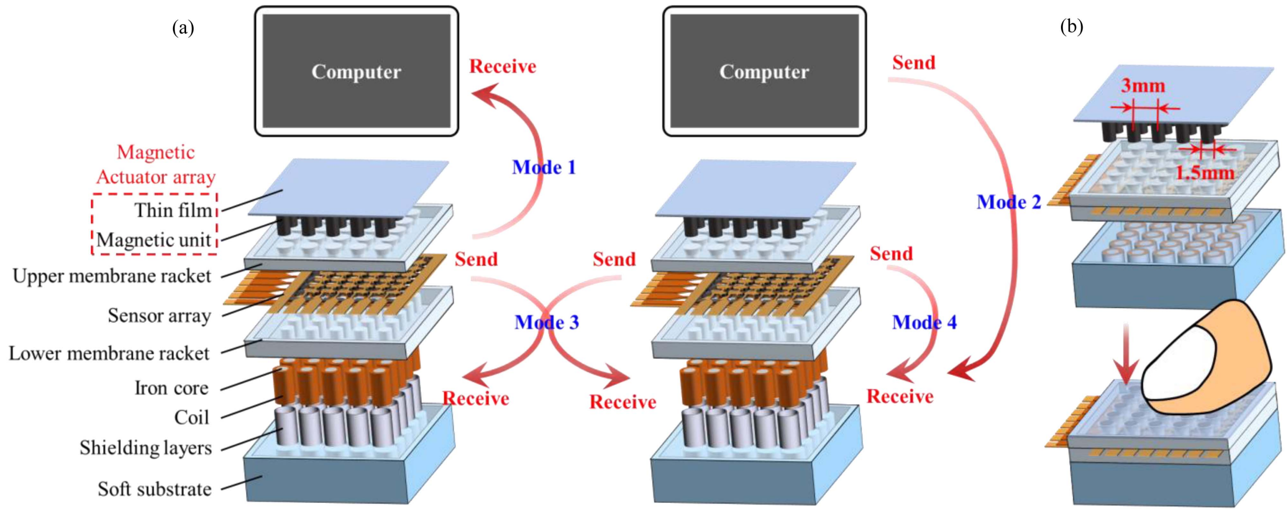

Fig. 2. Overall architecture of the proposed tactile device. (a) Explosion diagram and four control modes of the proposed tactile device. (b) Integration process of the proposed tactile device.

(Fig. S9, Supplementary material). Then, the resistance variation is converted into the voltage value, which is transmitted to the Arduino microcontroller board (abbreviated as Arduino) through the I/O (Input/Output) ports. Subsequently, the Arduino controls the actuator chips through the inter-integrated circuit and I/O ports, and then activates the corresponding coil to drive the magnetic actuator (see Fig. S10, Supplementary material).

For our tactile device, there are four control modes for different application scenarios. In mode 1, the proposed tactile device can be used as a sensing device to measure the interaction signals, such as pressure and touching location, and transmit them to a computer. Similarly, our proposed tactile device can receive the control signals from a computer and present different tactile information (mode 2). In addition, our proposed tactile device can modulate the actuator through sensing signals (modes 3 and 4). When two tactile devices interact together, the sensing signals of one tactile device can be used to control the magnetic actuator of another tactile device, so as to achieve multiuser communication or collaboration (mode 3). Meanwhile, the magnetic actuator of a tactile device is controlled by its own sensors and then provides tactile feedback (mode 4). In addition, we evaluated the system delay of our tactile device, which depends on the response time of the tactile sensor, the processing time of the sensor control system, the serial transmission time, and the response time of the tactile actuator (e.g., at an actuation frequency of 200 Hz). In four modes, the system delay is about 24.81, 5.97, 30.47, and 30.16 ms, respectively.

IV. Experimental Characterization

A. Characterization of Magnetic Actuator

To characterize the performance of the magnetic actuator in the proposed tactile device, we conducted quantitative experiments on pit depth, response time, and repeatability of the magnetic actuator using a homemade experimental testbed (see Fig. S11, Supplementary material). In these experiments, a laser displacement sensor (HL-G103-S-J, Panasonic, Japan) was adopted to record the pit depth.

The pit depth is important to ensure that users can accurately perceive the tactile feedback provided by our tactile device. When the fabricated parameters are determined, the pit depth depends on the magnetic force between the coil and the magnetic actuator, which further is affected by the current drive of the coil. To explore the relationship between drive current and pit depth, five magnetic actuators were selected to apply different drive currents. At the same driving current, each magnetic actuator was repeatedly measured ten times. As depicted in Fig. 3(a), the pit depth of the magnetic unit is increased with the increase of the drive current of the coil. At a 1.2-A drive current, the average pit depth of the magnetic unit is about 0.53 mm.

In addition, the dynamic characteristics are also important indicators to investigate the performance of the magnetic actuator. When a 1.2-A drive current was applied to the coil, the magnetic actuator moved downward rapidly under the magnetic force, and the pit depth reached a maximum within 540 ms [see Fig. 3(b)]. After the coil was powered OFF, and returned to its initial state in about 540 ms. As shown in Fig. 3(c), three work cycles were employed to evaluate the repeatability and stability of the magnetic actuator. In each work cycle, the magnetic actuator could respond steadily to the drive current, and the response time and the pit depth remain nearly constant. At a drive current of 1.2 A, the pit depth decreases sharply with the increase of the drive frequency (as shown in Fig. S12, Supplementary material). When the drive frequency reaches the maximum (250 Hz), the pit depth is about 0.88 μm, which is greater than the minimum threshold of the fingertip [28], [29].

B. Characterization of Piezoresistive Sensor

To accurately evaluate the performance of the piezoresistive sensor in practical applications, the sample composed of the

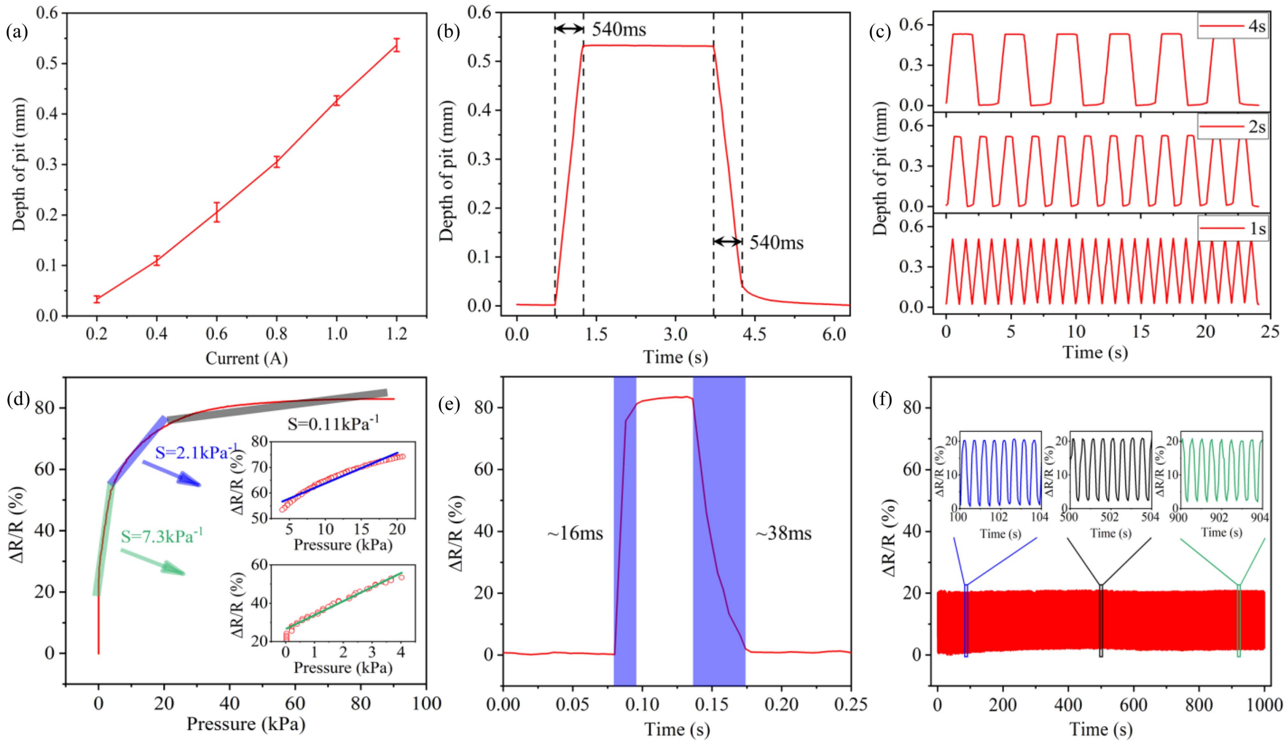

Fig. 3. Performance evaluation of magnetic actuator and piezoresistive sensor. (a) Pit depth of the magnetic actuator under different drive currents. (b) Response time of the magnetic actuator in one work cycle. (c) Repeatability of the magnetic actuator in 1000, 2000, and 4000 ms work cycles, respectively. (d) Sensitivity (abbreviated as S) of the piezoresistive sensor in different pressure. The insets show the sensitivity of the piezoresistive sensor in the low-pressure and medium-pressure regions. The green, blue and gray lines represent the sensitivity fitting curves of the three pressure regions respectively. (e) Response time of the piezoresistive sensor. (f) Fatigue test of the piezoresistive sensor. The insets present selected cycles at the beginning, middle, and end of the fatigue test.

magnetic actuator array, sensor array, and membrane brackets was tested using a dynamic testing system (ElectroPuls 1000, Instron, USA). The controllable pressure was applied to the sample by a three-dimensional printed cubic probe (10 mm^2 in the area) clamped on the dynamic testing system (see Fig. S13, Supplementary material), and the synchronous resistance measurement was performed by a digital multimeter (6500A, Keithley, USA).

Benefiting from the porous nature of TPU/CB sensing foam, the piezoresistive sensor has good sensitivity performance. The results of resistance as a function of pressure show that the overall response curve can be divided into three parts, as shown in Fig. 3(d). The fitted sensitivity of the piezoresistive sensor is about 7.3 kPa^{-1} in the low-pressure range of 0–4 kPa, about 2.1^{-1} kPa in the medium-pressure range of 4–20 kPa, and about 0.11 kPa^{-1} in the high-pressure range of 20–90 kPa.

As shown in Fig. 3(e), the piezoresistive sensor also exhibits a rapid response to external stress. For a given 50 kPa loading pressure, the resistance versus time curve shows a fast response and relaxation time of 16 and 38 ms, respectively. To assess the long-term repeatability of the piezoresistive sensor, a repetitive loading/unloading dynamic test was performed at a frequency of 0.5 Hz. During 2000 cycles, the resistance variation remains practically constant [see Fig. 3(f)], which indicates that the piezoresistive sensor has good fatigue characteristics.

C. Characterization of Tactile Device

In addition to external pressure, the piezoresistive sensor can also respond to vibrations from the magnetic actuator. Here, we investigated the characteristics of the piezoresistive sensor under different external pressures and different vibration frequencies of the magnetic actuator. The vibration frequency of the magnetic actuator is regulated by the work cycle of the drive current. An oscilloscope (UTD2152CEX, UNI-T, China) is adopted to measure the resistance of the piezoresistive sensor (see Fig. S14, Supplementary material).

Under four loaded states (external pressures), the magnetic actuator is activated by a drive current of a 1000-ms work cycle. With the increase of external pressure, the resistance variation of the piezoresistive sensor relative to the loaded state gradually decreases [see Fig. 4(a)]. In addition, the piezoresistive sensor is able to accurately respond and distinguish the vibrations of the magnetic unit when the coil is activated by the drive current of different work cycles [see Fig. 4(b)]. The Fourier transform of the resistance–time relation curve shows the frequency of the resistance variation is consistent with the frequency of the drive current, which also proves the accuracy of the piezoresistive sensor [see Fig. 4(c)]. At each vibration frequency of the magnetic actuator, the resistance variation of the piezoresistive sensor relative to the nonloaded state decreases sharply with the increase of the external pressure [see Fig. 4(d)]. Even

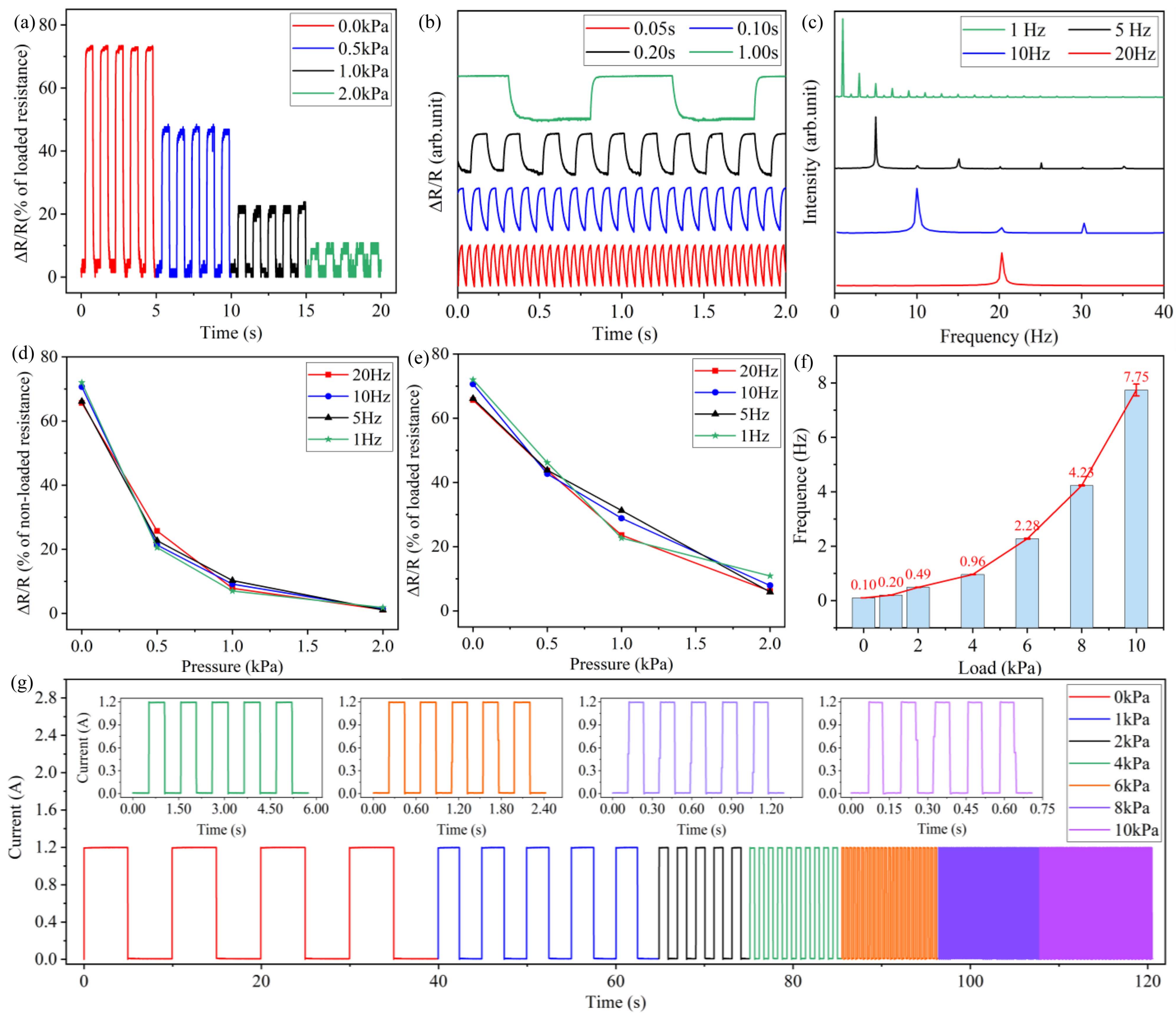

Fig. 4. Performance evaluation of the tactile device. (a) Response of the piezoresistive sensor to the 1-Hz vibration of the magnetic actuator under different loaded states. (b) And (c) the time domain/frequency domain response of the piezoresistive sensor to the vibration of the magnetic actuator at different frequencies of the drive current. (d) And (e) relationship between the resistance variation of the piezoresistive sensor relative to the nonloaded/loaded state and the external pressure and the vibration frequency of the magnetic actuator. (f) Mapping relationship between the applied loads and frequency of the drive current. (g) Work cycle of the drive current at different applied pressure.

the resistance variation relative to the loaded state decreases approximately linearly with increasing external pressure [see Fig. 4(e)]. These results indicate that the vibration frequency of the magnetic actuator has little effect on the sensor's sensing of external pressure.

Moreover, we investigated the feasibility of variable-frequency control of our tactile device. An exponential function is used to map the external pressure to the work cycle of the drive current. Several pressures (i.e., 0 , 1, 2, 4, 6, 8, and 10 kPa) are applied to the tactile device, and a digital power meter (Gravity, DFRobot, China) is adopted to record the drive current of the coil (see Fig. S15, Supplementary material). As shown in Fig. 4(g), the work cycle of the drive current decreases with the increase of the pressure. Since the vibration frequency of the magnetic actuator is consistent with the frequency of the drive current [see Fig. 4(f)], the variable-frequency movement of the magnetic actuator can be realized by applying different pressures, so as to provide different vibration stimuli to the user. During vibration, the maximum output force of the magnetic actuator is about 34 mN (see Fig. S16 and S17, Supplementary material). Furthermore, we developed an experimental setup to evaluate the collaborative operation ability of the proposed tactile device, and the experimental results indicate that the tactile actuator and tactile sensor can work together at the same time under external pressure (see Figs. S18 and S19, Supplementary material).

V. Application of Tactile Device

To better understand the effectiveness of our proposed tactile device and its different control modes, we developed three

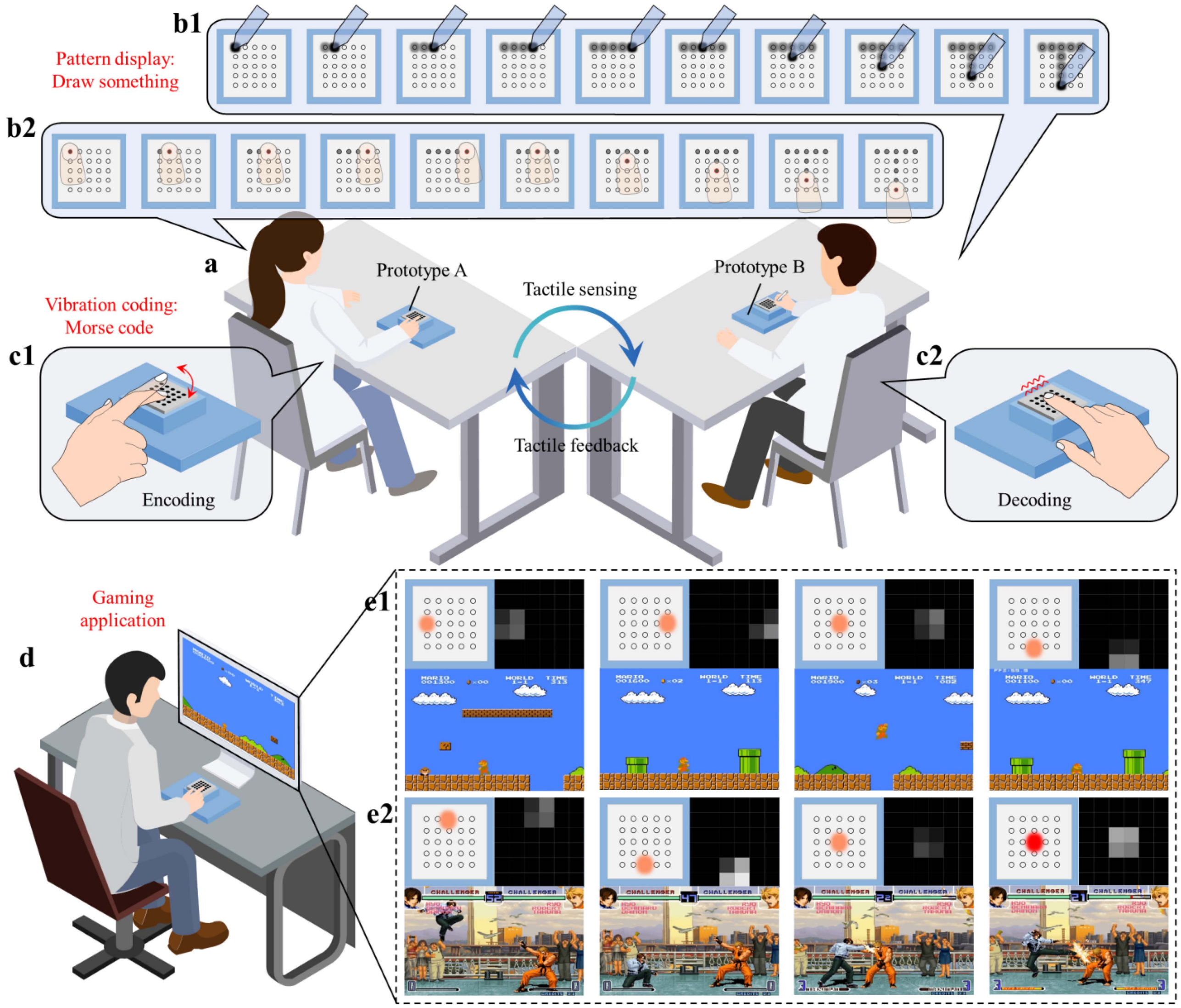

Fig. 5. Application of the tactile device. (a) Transmission of patterns and vibration flows between two users. (b1) And (b2) draw something. The boy writes on the tactile device using a common pen, while the girl distinguishes the formulated pattern on another tactile device. (c1) And (c2) morse code. The girl encodes the transmission signal by pressuring the tactile device at different frequencies, and the boy could perceive the vibration signals on the other device. (d) Gaming applications. Orange and red circles denote light and strong touch, and the white square denotes the touch position on the sensors. (e1) When touching the left, right, center, and bottom of the tactile device, Mario moves left, right, jumps and squats. (e2) The character of the king of fighters will jump, squat, and punch/kick while touching the top, bottom, and center of the tactile device. When the character punches and kicks (i.e., a light touch and a strong touch), the user can perceive the low-frequency and high-frequency vibration provided by the tactile device, respectively.

representative applications, namely the pattern display, vibration coding, and games. As shown in Fig. 5(a), each standalone tactile device can play the role of sensing or feedback during the interaction between two users (mode 3). When one user [the boy in Fig. 5(a)] draws a pattern on prototype B using a common pen or finger, the touching location is recorded by the sampling circuit [see Fig. 5(b1)]. According to the recorded positions, the drive system commands prototype A to formulate the same pattern, and the other user [the girl in Fig. 5(a)] can perceive it by fingers [see Fig. 5(b2)].

Similar to the pattern, vibration is also an effective way to transmit tactile information. When a user touches the prototype, the touch duration is recorded and transformed to different vibration frequencies. By varying the touch duration, vibration signals of different frequencies are combined into vibration flow to realize the transmission of tactile information. The short-period and long-period touch are set to dot and dash in Morse code, respectively, corresponding to the high-frequency and low-frequency vibrations in tactile feedback. For example, when the girl touches prototype A in the order of three short periods, three long periods, and three short periods [see Fig. 5(c1) and video], the interaction information is encoded as "SOS" in Morse code. Subsequently, prototype B recreates this interaction information for the boy with the same vibration frequency and vibration sequence [see Fig. 5(c2) and video].

In the above interaction scenarios (Draw something and Morse code), mode 3 mentioned in Section III-B is adopted. Through this control mode, different patterns or vibration flows can be transmitted between two or more users, realizing the transmission and sharing of tactile information. For the tactile device, mode 2 is a traditional control mode, which has been demonstrated in our previous study [26]. Expect for mode 3 and mode 2, the other two modes are presented through the game applications.

As depicted in Fig. 5(d), the user interacts with the prototype on the table and controls the actions of the virtual character in the games through different touch signals. When the user touches the left, right, center, and bottom of the prototype [see orange circles in Fig. 5(e1)], these locations are recorded by the sensors of the prototype [see white squares in Fig. 5(e1)] and mapped to Mario's actions in the computer. In Super Mario, only the tactile sensing of the prototype is used to transmit the interaction information to the computer (mode 1). Furthermore, we integrate mode 1 and mode 4 into the King of Fighters to present the capability of actuating and sensing within the compact contact area of a fingertip [see Fig. 5(e2) and video]. The movements of the character in the computer can be controlled by the touching location (mode 1). When a light touch (orange circle) or strong touch (red circle) is applied to the center of the prototype, the character in the computer punches or kicks, while the user can perceive the low-frequency or high-frequency vibration provided by the prototype in real time (mode 4). Compared with traditional game controllers, tactile devices with tactile sensing can greatly improve the interactive immersion of games.

VI. Conclusion

In this article, we propose a reticular sandwich structure for developing a high-resolution tactile device with both tactile display and tactile sensing. The proposed reticular sandwich structure effectively avoids interference from the sensors to the actuators, while also compacting the actuator and sensor array, enabling the actuating–sensing integrated tactile device to meet the spatial registration requirement. Experiments show that the proposed tactile device can act as a communicator or game controller, and has the potential to be used across a wide range of applications pertaining to intelligent vehicles (see Fig. S20, Supplementary material), virtual reality, teleoperation, social media, etc.

In the future, we will develop a fitted model to characterize the relationship between the external pressure, vibration frequency, and resistance variation, and then realize the monitoring of the actuator motion state and precise control of the actuator vibration frequency in the interaction process. Additionally, we plan to apply this device to the information communication between visually impaired and sighted people through synchronized tactile reproduction of graphs and text [30].

References

[1] R. A. Norman and R. Menendez, "Structure and function of aging skin," in *Diagnosis of Aging Skin Diseases*, R. A. Norman, Ed. Berlin, Germany: Springer-Verlag, 2008, pp. 5–10, doi: 10.1007/978-1-84628-678-0_2.

[2] R. Pfeifer, M. Lungarella, and F. Iida, "The challenges ahead for bio-inspired 'soft' robotics," *Commun. Assoc. Comput. Machinery*, vol. 55, no. 11, pp. 76–87, Nov. 2012, doi: 10.1145/2366316.2366335.

[3] R. Balasubramanian and V. J. Santos, Eds., "The human hand as an inspiration for robot hand development," in *Springer Tracts in Advanced Robotics*, vol. 95. Berlin, Germany: Springer-Verlag, 2014, doi: 10.1007/978-3-319-03017-3.

[4] A. C. Guyton and J. E. Hall, *Textbook of Medical Physiology*, 6th ed. Philadelphia, PA, USA: Saunders, 1981.

[5] A. K. Han, S. Ji, D. Wang, and M. R. Cutkosky, "Haptic surface display based on miniature dielectric fluid transducers," *IEEE Robot. Automat. Lett.*, vol. 5, no. 3, pp. 4021–4027, Jul. 2020.

[6] N. Torras et al., "Tactile device based on opto-mechanical actuation of liquid crystal elastomers," *Sens. Actuators A, Phys.*, vol. 208, pp. 104–112, Feb. 2014, doi: 10.1016/j.sna.2014.01.012.

[7] R. H. Heisser et al., "Valveless microliter combustion for densely packed arrays of powerful soft actuators," *Proc. Nat. Acad. Sci. USA*, vol. 118, no. 39, Sep. 2021, Art. no. e2106553118, doi: 10.1073/pnas.2106553118.

[8] X. Qu et al., "Refreshable braille display system based on triboelectric nanogenerator and dielectric elastomer," *Adv. Funct. Mater.*, vol. 31, no. 5, Jan. 2021, Art. no. 2006612, doi: 10.1002/adfm.202006612.

[9] S. Yun et al., "Polymer-based flexible visuo-haptic display," *IEEE/ASME Trans. Mechatron.*, vol. 19, no. 4, pp. 1463–1469, Aug. 2014.

[10] Y. Liu et al., "Electronic skin as wireless human-machine interfaces for robotic VR," *Sci. Adv.*, vol. 8, no. 2, Jan. 2022, Art. no. eabl6700, doi: 10.1126/sciadv.abl6700.

[11] S. H. Yoon et al., "HapSense: A soft haptic I/O device with uninterrupted dual functionalities of force sensing and vibrotactile actuation," in *Proc. 32nd Annu. Assoc. Comput. Machinery Symp. User Interface Softw. Technol.*, 2019, pp. 949–961, doi: 10.1145/3332165.3347888.

[12] O. Ozioko, P. Karipoth, M. Hersh, and R. Dahiya, "Wearable assistive tactile communication interface based on integrated touch sensors and actuators," *IEEE Trans. Neural Syst. Rehabil. Eng.*, vol. 28, no. 6, pp. 1344–1352, Jun. 2020.

[13] O. Ozioko, W. Taube, M. Hersh, and R. Dahiya, "SmartFingerBraille: A tactile sensing and actuation based communication glove for deafblind people," in *Proc. IEEE 26th Int. Symp. Ind. Electron.*, 2017, pp. 2014–2018, doi: 10.1109/ISIE.2017.8001563.

[14] J.-H. Youn, I. B. Yasir, and K.-U. Kyung, "Self-sensing soft tactile actuator for fingertip interface," in *Proc. IEEE/RSJ Int. Conf. Intell. Robots Syst.*, 2020, pp. 8939–8944, doi: 10.1109/IROS45743.2020.9341087.

[15] C. Suh, J. C. Margarit, Y. S. Song, and J. Paik, "Soft pneumatic actuator skin with embedded sensors," in *Proc. IEEE/RSJ Int. Conf. Intell. Robots Syst.*, 2014, pp. 2783–2788, doi: 10.1109/IROS.2014.6942943.

[16] S. S. Robinson et al., "Integrated soft sensors and elastomeric actuators for tactile machines with kinesthetic sense," *Extreme Mechanics Lett.*, vol. 5, pp. 47–53, Dec. 2015, doi: 10.1016/j.eml.2015.09.005.

[17] J. Chen, B. Chen, K. Han, W. Tang, and Z. L. Wang, "A triboelectric nanogenerator as a self-powered sensor for a soft–Rigid hybrid actuator," *Adv. Mater. Technol.*, vol. 4, no. 9, Sep. 2019, Art. no. 1900337, doi: 10.1002/admt.201900337.

[18] O. Ozioko, P. Karipoth, P. Escobedo, M. Ntagios, A. Pullanchiyodan, and R. Dahiya, "SensAct: The soft and squishy tactile sensor with integrated flexible actuator," *Adv. Intell. Syst.*, vol. 3, no. 3, Mar. 2021, Art. no. 1900145, doi: 10.1002/aisy.201900145.

[19] D. Li et al., "Touch IoT enabled by wireless self-sensing and haptic-reproducing electronic skin," *Sci. Adv.*, vol. 8, no. 51, Dec. 2022, Art. no. eade2450, doi: 10.1126/sciadv.ade2450.

[20] M. Zhu et al., "Haptic-feedback smart glove as a creative human-machine interface (HMI) for virtual/augmented reality applications," *Sci. Adv.*, vol. 6, no. 19, May 2020, Art. no. eaaz8693, doi: 10.1126/sciadv.aaz8693.

[21] X. Guo, Y. Zhang, D. Wang, L. Lu, J. Jiao, and W. Xu, "The effect of applied normal force on the electrovibration," *IEEE Trans. Haptics*, vol. 12, no. 4, pp. 571–580, Oct./Dec. 2019.

[22] N. H. L. Vuong et al., "Active skin as new haptic interface," *Proc. SPIE*, vol. 7642, Mar. 2010, Art. no. 76422M, doi: 10.1117/12.847230.

[23] P. M. Khin et al., "Soft haptics using soft actuator and soft sensor," in *Proc. IEEE 6th Int. Conf. Biomed. Robot. Biomechatron.*, 2016, pp. 1272–1276, doi: 10.1109/BIOROB.2016.7523806.

[24] K. Kadooka, H. Imamura, and M. Taya, "Tactile sensor integrated dielectric elastomer actuator for simultaneous actuation and sensing," *Proc. SPIE*, vol. 9798, Apr. 2016, Art. no. 97982H, doi: 10.1117/12.2218779.

[25] H. Phung, P. T. Hoang, H. Jung, T. D. Nguyen, C. T. Nguyen, and H. R. Choi, "Haptic display responsive to touch driven by soft actuator and soft sensor," *IEEE/ASME Trans. Mechatron.*, vol. 26, no. 5, pp. 2495–2505, Oct. 2021.

[26] Y. Guo, Q. Tong, P. Zhao, Y. Zhang, and D. Wang, "Electromagnetic-actuated soft tactile device using a pull–push latch structure," *IEEE Trans. Ind. Electron.*, vol. 70, no. 10, pp. 10344–10352, Oct. 2023.

[27] N. Liang, C. Shang, Q. Xu, Y. Li, and Z. Peng, "A deformable fingertip sensor assists the manipulator in distinguishing the hardness of the object," in *Proc. IEEE Int. Flexible Electron. Technol. Conf.*, 2022, pp. 1–2, doi: 10.1109/IFETC53656.2022.9948519.

[28] S. M. Petermeijer, J. C. F. de Winter, and K. J. Bengler, "Vibrotactile displays: A survey with a view on highly automated driving," *IEEE Trans. Intell. Transp. Syst.*, vol. 17, no. 4, pp. 897–907, Apr. 2016.

[29] L. A. Jones and N. B. Sarter, "Tactile displays: Guidance for their design and application," *Hum. Factors*, vol. 50, no. 1, pp. 90–111, Feb. 2008, doi: 10.1518/001872008X250638.

[30] J. C. Koone et al., "Data for all: Tactile graphics that light up with picture-perfect resolution," *Sci. Adv.*, vol. 8, no. 33, Aug. 2022, Art. no. eabq2640, doi: 10.1126/sciadv.abq2640.

Yuan Guo (Member, IEEE) received the Ph.D. degree in mechanical engineering from Beihang University, Beijing, China, in 2023.

He is currently working as the Postdoctoral Fellow in the Biomedical Engineering, City University of Hong Kong, Hong Kong. His research interests include haptics, human–machine interaction, force feedback glove, VR, and robotics.

Chao Shang received the Ph.D. degree in condense matter physics from the University of Science and Technology of China, Hefei, China, in 2019. He is currently working as the Postdoctoral with the School of Physics and Optoelectronic Engineering, Shenzhen University, Shenzhen, China. His research interests include hydrogel, additive manufacturing, electronic skin, and deep learning.

Qianqian Tong (Member, IEEE) received the Ph.D. degree in computer application technology from Wuhan University, Wuhan, China, in 2019.

She is currently an Associate Researcher with Peng Cheng Laboratory, Shenzhen, China. Her research interests include haptic rendering, haptic human-machine interface, and medical imaging analysis.

Yuru Zhang (Senior Member, IEEE) received the Ph.D. degree in mechanical engineering from Beihang University, Beijing, China, in 1987.

She is currently a Professor with the State Key Laboratory of Virtual Reality Technology and Systems, Beihang University. Her technical interests include haptic human–machine interface, medical robotic systems, robotic dexterous manipulation, and virtual prototyping.

Dr. Zhang is a member of ASME.

Zhengchun Peng received the B.S. degree in mechanical engineering from the Beijing Institute of Technology, Beijing, China, and the Ph.D. degree in MEMS from the Georgia Institute of Technology, Atlanta, GA, USA, in 2011.

He then joined Intel Corp. as a Senior R&D Engineer, developing Wafer Sort and E-Test technologies for 14 and 10 nm processors. He is currently a distinguished Professor with Shenzhen University, Shenzhen, China. His main research interests include the fields of micro/nanosensors, flexible/stretchable electronics, and their application in robotics, human–machine interface, and healthcare.

Dangxiao Wang (Senior Member, IEEE) received the Ph.D. degree in mechanical engineering from Beihang University, Beijing, China, in 2004.

He is currently a Professor with the State Key Laboratory of Virtual Reality Technology and Systems, Beihang University. From 2006 to 2016, he was an Assistant and Associate Professor with the School of Mechanical Engineering and Automation, Beihang University. His research interests include haptic device, haptic rendering, and medical robotic systems.

Dr. Wang was an Associate Editor for IEEE TRANSACTIONS ON HAPTICS from 2015 to 2018. He had been the Chair of Executive Committee of the IEEE TECHNICAL COMMITTEE ON HAPTICS from 2014 to 2017.